Ultrasonic-assisted synthesis and characterization of semiconductor CuO nanoparticles via decomposition of ethanedioate precursor

Ahmad Rahnama[1,2], Mehrnaz Gharagozlou[1*]

[1]Department of Nanotechnology and Nanomaterials, Institute for Color Science and Technology, P.O. Box 16765-654 Tehran, (IRAN)
[2]Azad University, Shahr-e-Rey Branch, Tehran, (IRAN)
E-mail: gharagozlou@icrc.ac.ir

Received: 14th June, 2011 ; Accepted: 14th July, 2011

ABSTRACT

Semiconductor cupric oxide nanoparticles are of great interest due to their numerous applications in many important fields of science and technology such as pigments, semiconductors, sensors, catalysts and solar cells. In this work, nanoparticles of semiconductor cupric oxide with an average size of 52 nm have been successfully synthesized via ultrasonic-assisted thermal decomposition of the ethanedioate precursor at 400 °C. The nanoparticles were characterized by powder X-ray diffraction (XRD), FT-IR spectroscopy, scanning electron microscopy (SEM), transmission electron microscopy (TEM), colorimetric analysis ($L^*a^*b^*$ color parameters), diffuse reflectance spectroscopy and UV-Vis spectroscopy. Our results confirmed the formation of the pure single-phase monoclinic cupric oxide (space group C2/c) with the monoclinic structure. The FT-IR spectrum displays the typical vibration of cupric oxide at 536 cm^{-1}. Also the optical absorption spectrum indicates that the cupric oxide nanoparticles have a direct band gap of 1.95 eV, which is larger than the reported value for the bulk cupric oxide (1.85 eV).
© 2012 Trade Science Inc. - INDIA

INTRODUCTION

Metal oxide nanoparticles have been actively studied for their size- and shape-induced novel properties. In recent years, the synthesis and production of semiconductor metal oxide nanoparticles has received much attention due to their excellent physical and chemical properties in comparison to their bulk counterparts, and also their potential applications in nanoscale devices as interconnectors for nanoelectronics[1-3].

Among these materials, cupric oxide, a p-type semi-conductor with a narrow band gap, has been studied intensely because of its numerous applications in catalysis, pigments, semiconductors, batteries, sensors and field transistors[4-7]. On the other hand, the large fractions of surface area, excellent stability and good electric properties have guided to new studies to determine its applicability as a suitable material for solar cells, in particular due to its photoconductivity and photochemical properties[8]. Also nanocrystalline p-type semiconductor cupric oxide is of special interest because of its efficiency as nanofluids in heat-transfer applications. It

Full Paper

has been reported that 4% addition of this compound improves the thermal conductivity of water by 20%.

Ultrasound is a very effective processing method in the generation and application of nanosized materials. In general, ultrasonic cavitation in liquids may cause fast and complete degassing: initiate various chemical reactions by generating free chemical ions (radicals); accelerate chemical reactions by facilitating the mixing of reactants; enhance polymerization and depolymerization reactions by temporarily dispersing aggregates or by permanently breaking chemical bonds in polymeric chains; increase emulsification rates; improve diffusion rates; produce highly concentrated emulsions or uniform dispersions of micron-size or nanosized materials; assist the extraction of substances such as enzymes from animal, plant, yeast, or bacterial cells; remove viruses from infected tissue; and finally, erode and break down susceptible particles, including micro-organisms[2].

Today, many nanomaterials are produced in a dry process. As a result, the particles need to be mixed into liquid formulations. This is where most nanoparticles form agglomerates during the wetting. Therefore effective means of deagglomerating and dispersing are required to overcome the bonding forces after wettening the micropowder or nanopowder.

Some methods for the preparation of nanocrystalline p-type metal oxide semiconductors have been reported recently such as sol-gel technique, one-step solid state reaction method at the room temperature, electrochemical method, thermal decomposition of precursors and co-implantation of metal and oxygen ions[7-10]. Conventional methods for the preparation of cupric oxide include one step solid state reaction at the room temperature, mechanical milling of commercial powders, and so on. However, none of these methods seems to be suitable for the preparation of highly dispersed cupric oxide nanoparticles, which has been found to be an obstacle to many applications, especially in catalysts and electrodes.

Despite considerable efforts have been devoted to the preparation of nanocrystalline p-type semiconductor cupric oxide[4-10], there is a lack of information about the preparation of the semiconductor cupric oxide via ultrasonic-assisted decomposition of the ethanedioate precursor.

In the present work, we report on the synthesis and characterization of semiconductor nanoparticles via a novel method based on the ultrasonic-assisted decomposition of the ethanedioate precursor. Some advantages of the method are mild conditions of reaction and non toxic aqueous solvents.

EXPERIMENTAL

All the reagents were analytical grade and were used without further purification. In a typical process, $Cu(NO_3)_2.3H_2O$ was dissolved in deionized water to form a transparent solution, and then used the ultrasonic irradiation for 30 min. Subsequently 5 mmol ethanedioate acid dissolved in an equal volume of deionized water and added dropwise to the above solution under the ultrasonic irradiation. The suspension cooled in the room temperature. After washed with deionized water and ethanol for three times to purify the product, the precipitate of the precursor was centrifuged and dried at 55 ºC for 14 h. Then cupric ethanedioate precursor was heated to 400 ºC (rate of 5 ºC min^{-1}) and calcined at this temperature for 3 h in the ambient atmosphere.

The ultrasonic irradiation processor was a Hielscher UP400S (400W, 24 kHz). FT-IR spectra (500-4000 cm^{-1}) were recorded on a Perkin Elmer Spectrum One spectrophotometer with KBr pellets. Thermal analyses (TG-DTG-DTA) were carried out using a Perkin Elmer simultaneous thermal analyzer (STA Pyris Diamond Model) with the heating rate of 5°C/min in flowing air. X-ray diffraction (XRD) was performed on a Philips PNA-analytical diffractometer using CuKα radiation. The SEM micrograph was obtained on a LEO 1455VP scanning electron microscope. The transmission electron microscopy (TEM) image was obtained using a Philips CM-120. Measurement of $L^*a^*b^*$ color parameters and diffuse reflectance spectrum were carried out on a spectrophotometer CE-7000A, in the 350-750 nm range using the D65 illumination.

RESULTS AND DISCUSSION

In Figure 1 XRD pattern for cupric oxide nanoparticles is displayed. All of diffraction peaks corresponds to the cupric oxide monoclinic phase and are agreement with JCPDS 41-0254 card. There are not

any peaks of impurity in the XRD pattern. The average crystalline size of the prepared cupric oxide particles is estimated to be 45 nm according to the Debye-Scherrer equation (1).

$$t = \frac{0.9\lambda}{\beta \cos\theta} \qquad (1)$$

where t is the crystallite size, λ the wavelength of X-ray radiation (CuKα), θ the Bragg angle and β is the full width at half maximum (FWHM) of the most intense diffraction peak.
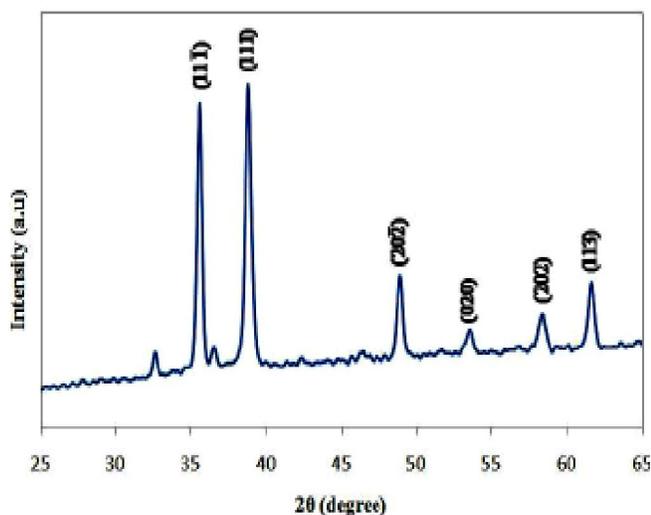

Figure 1 : XRD pattern of cupric oxide nanoparticles.

Figure 2 : Thermal analyses of the cupric ethanedioate precursor (a) TG-DTA and (b) TG-DTG.

Figure 2 shows the simultaneous thermal analyses (TG-DTG-DTA) of the as-prepared cupric ethanedioate precursor. The thermogravimetery (TG) and derivative thermogravimetery (DTG) curves show the weight loss. There is a weight loss step in the temperature ranges 270-330 °C. which may be ascribed to the decomposition of the ethanedioate accompanied by the exothermic peak in the differential thermal analysis (DTA) curve. The weight loss is about 45 %, which is close to the theoretical value. Above 400 °C the weight loss is negligible. The DTA curve exhibits a large exothermic peak around 300 °C which can be ascribed to the burn out of the ethanedioate. It confirms that the majority of the mass loss occurs under 400 °C and allows for optimization of the heat treatment program.

The FT-IR spectra of the cupric ethanedioate precursor and cupric oxide nanoparticles were shown in Figure 3 and 4. In the FT-IR spectrum of the precursor (Figure 3), peaks observed at around 1626 and 1363 cm^{-1} are related to the asymmetric ν_{as}(COO) and sym-
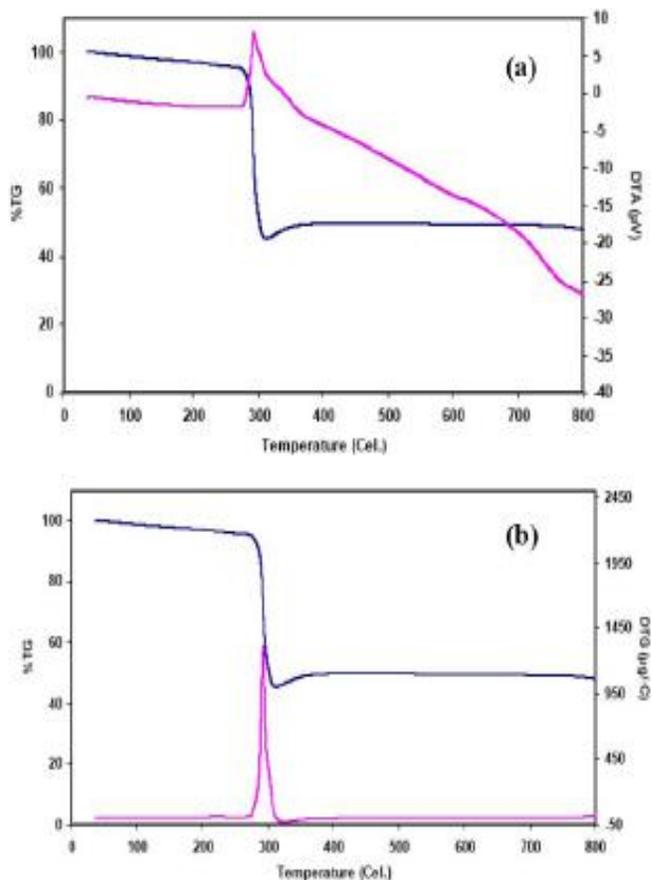
metric ν_s(COO) stretching vibration of COO groups, respectively which corroborate the coordination of metal ions by carboxylates groups to form a complex. This gives rise to a large difference between ν_{as}(COO) and ν_s(COO), $\Delta\nu$ (ν_{as}(COO)-ν_s(COO)) of about 263 cm^{-1}, characteristic of the monodentate coordination of carboxylate groups to the metal ions[10] which confirms the ethanedioate precursor.

While, in the FT-IR spectrum of the cupric oxide nanoparticles (Figure 4), the absence of some of the organic bands could be ascribed to the complete decomposition of the organic compounds. There is an obvious absorption peak at around 536 cm^{-1} that was the result of overlap of two peaks, which can be assigned to the vibrations of Cu-O bands.

SEM image of the as-prepared cupric oxide nanoparticles is presented in Figure 5, showing that the morphology of particles was nearly spherical and regular in the shape.

Figure 6. demonstrated the TEM micrograph and selected area electron diffraction (SAED) pattern of
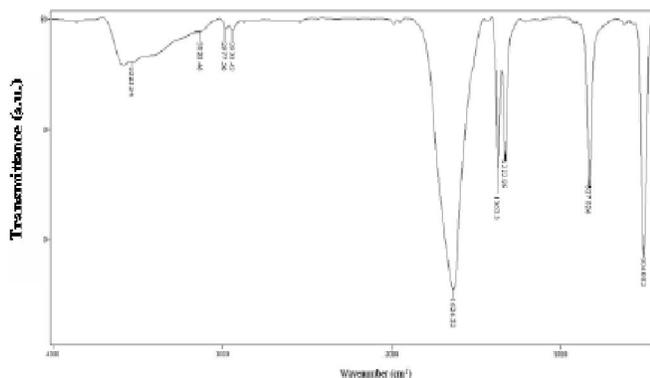
Full Paper

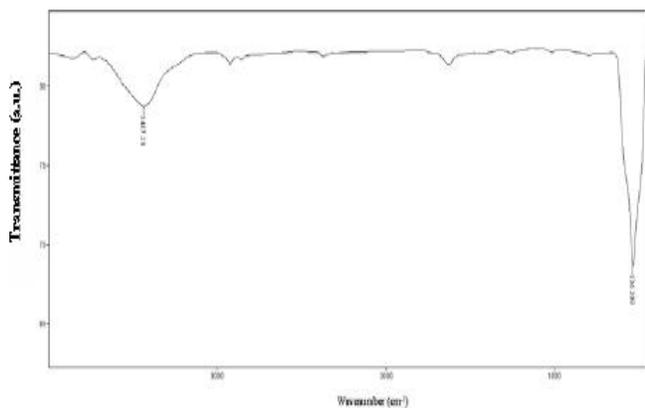**Figure 3 : FT-IR spectrum of the cupric ethanedioate precursor.**
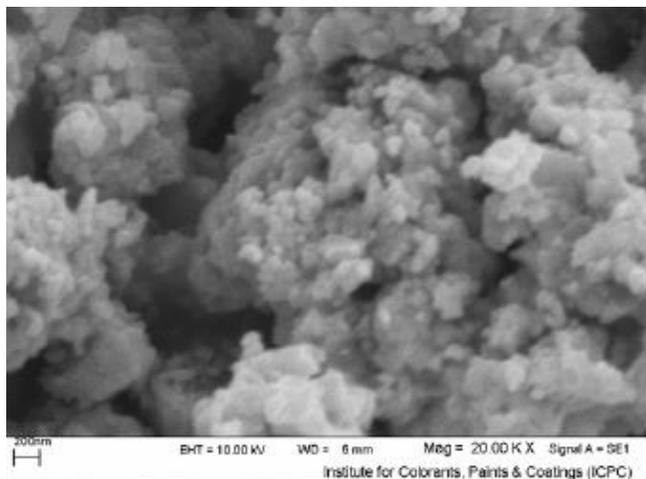

Figure 4 : FT-IR spectra of cupric oxide nanoparticles.

Figure 5 : SEM micrograph of cupric oxide nanoparticles.

Figure 6 : TEM micrograph (a) and SAED pattern (b) of cupric oxide nanoparticles.

cupric oxide nanoparticles, presetting that the product composed of almost spherical nanoparticles with the average particle sizes of 52 nm, which is in good agreement with that estimated by the Scherrer equation from XRD pattern. The different lattice planes in the SAED patterns (Figure 6b) are in good agreement with the present monoclinic system.
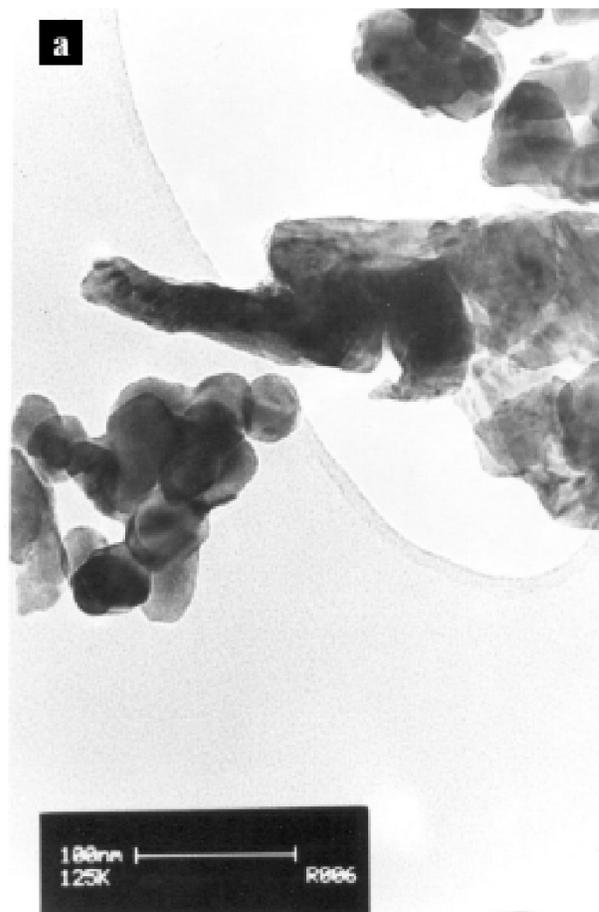
The optical absorption spectrum of cupric oxide nanoparticles showed in Figure 7. For measurements, the cupric oxide product is dispersed in the deionized water by the ultrasonic irradiation. There is a broad absorption peak at about 360 nm which is in good agreement with the previous reports[9, 11].
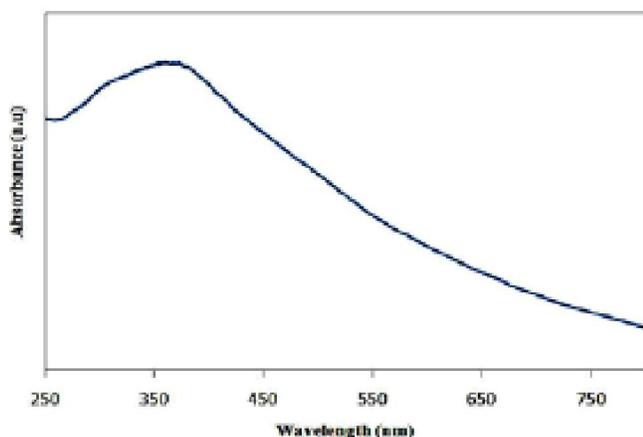
The absorption band gap E_g can be determined by

Full Paper

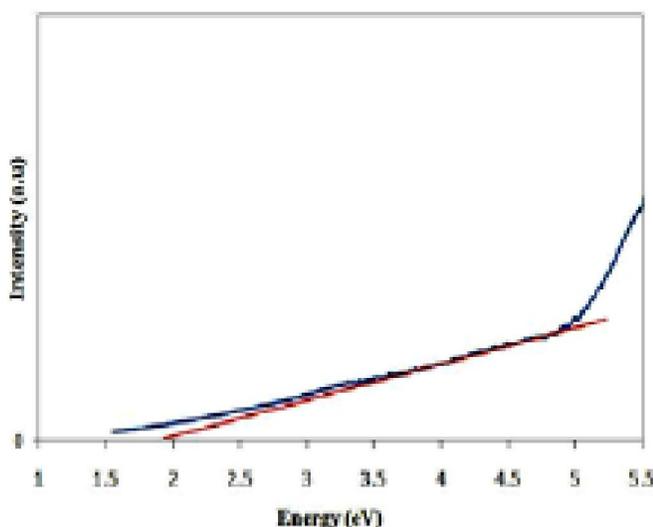**Figure 7 : Optical absorption spectrum of cupric oxide nanoparticles.**

Figure 8 : $(\alpha h\nu)^2$ versus $h\nu$ curve of the semiconductor sample.

the following equation (2):

$$(\alpha h\nu)^n = B(h\nu - E_g) \qquad (2)$$

where $h\nu$ is the photo energy, α is the absorption coefficient, B is a constant relative to the material and n is either 2 for a direct transition or 1/2 for an indirect transition[12]. The band gap of the as-obtained cupric oxide is estimated to be 1.95 eV that is larger than the reported value for the bulk cupric oxide (1.85 eV). Figure 8 shows the $(\alpha h\nu)^2$ versus $h\nu$ curve for the sample. Compared to previous reports[9] in our ultrasonic-assisted preparation method the band gap significantly decreased to 1.95 eV.

The color of cupric oxide was evaluated from $L^*a^*b^*$ colorimetric coordinates and diffuse reflectance spectroscopy. The CIE-$L^*a^*b^*$ colorimetric method as recommended by the Commission Internationale I′Eclairage

(CIE) standards was used to measure the $L^*a^*b^*$ color parameters of cupric oxide. In this method, L^* varies from black (0) to white (100), b^* from blue (-) to yellow (+) and a^* from green (-) to red (+). Values of the colorimetric data L^*, a^* and b^* were found to be 11.01, 1.92 and 4.51, respectively.

The diffuse reflectance spectrum of cupric oxide is shown in Figure 9. Results from diffuse reflectance spectroscopy revealed nearly complete light absorption due to the very low intensity of the reflection in the 350-750 nm range. This was further confirmed by the colorimetric coordinates. The relatively low values of L^*, a^* and b^* suggested full light absorption and confirmed the black color of cupric oxide which are in agreement with the color matched with the obtained $L^*a^*b^*$ color parameters.
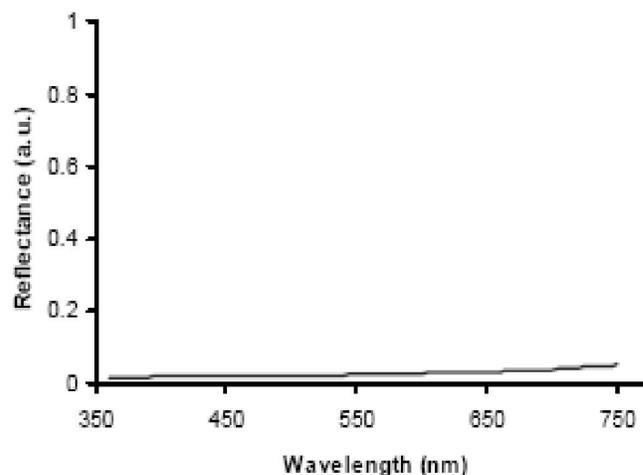

Figure 9 : Diffuse reflectance spectrum of cupric oxide nanoparticles.

CONCLUSION

In summary, nanoparticles of semiconductor cupric oxide have been successfully synthesized via ultrasonic-assisted thermal decomposition of ethanedioate precursor at 400 °C. The average size of nanoparticles was about 52 nm with the almost spherical morphology. The optical absorption band gap of the sample is determined to be 1.95 eV, which is larger than the reported value for the bulk material (1.85 eV). We hope that this ultrasonic-assisted synthesis route can be extended to prepare other systems involving other metal oxides.

Full Paper

ACKNOWLEDGEMENTS

REFERENCES

[1] Y.Xia, P.Yang, Y.Sun, Y.Wu, B.Mayers, B.Gates, Y.Yin, F.Kim, H.Yan; Adv.Mater., **15**, 353-389 **(2003)**.

[2] P.P.Edwards, C.N.R.Rao, G.U.Kulkarni, P.J.Thomas; Chem.Eur.J., **8**, 29-35 **(2002)**.

[3] W.Wang, I.N.Germanenko, M.S.El-Shall; Chem.Mater., **14**, 3028-3033 **(2002)**.

[4] A.Chowdhuri, V.Gupta, K.Sreenivas, R.Kumar, S.O.Mozumdar, P.K.Patanjali; Appl.Phys.Lett., **84**, 1180-1182 **(2004)**.

[5] G.L.Luquea, M.C.Rodrígueza, G.A.Rivas; Talanta., **66**, 467-471 **(2005)**.

[6] A.Umar, M.M.Rahman, A.Al-Hajry, Y.B.Hahn; Electrochem.Commun., **11**, 278-281 **(2008)**.

[7] X.G.Zheng, C.N.Xu, Y.Tomokiyo, E.Tanaka, H.Yamada, Y.Soejima; Phys.Rev.Lett., **85**, 5170-5173 **(2000)**.

[8] R.A.Zaratea, F.Heviab, S.Fuentesa, V.M.Fuenzalidac, A.Zunigad; J.Solid State Chem., **180**, 1464-1469 **(2007)**.

[9] X.Zhang, D.Zhang, X.Ni, H.Zheng; Solid-State Electron, **52**, 245-248 **(2008)**.

[10] D.Li, Y.H.Leung, A.B.Djurišić, Z.T.Liu, M.H.Xie, J.Gao, W.K.Chan; J.Cryst.Growth, **282**, 105-111 **(2005)**.

[11] M.Kaur, K.P.Muthe, S.K.Despande, S.Choudhury, J.B.Singh, N.Verma, S.K.Gupta, J.V.Yakhmi; J.Cryst.Growth, **289**, 670-675 **(2006)**.

[12] C.T.Hsieh, J.M.Chen, H.H.Lin, H.C.Shih; Appl.Phys.Lett., **83**, 3383-3385 **(2003)**.